Influence of cutting flutes on stress distribution for selected dental implants: Numerical studies

Pankaj Dhatrak [a],*, Uddhav Shirsat [b], S. Sumanth [c], Vijay Deshmukh [d]

[a] Faculty of Mechanical Engineering, Dr. Vishwanath Karad MIT-WPU(Formerly MAEER'S MIT Pune), Pune 411038, India
[b] Faculty of Mechanical Engineering, Bhivarabai Sawant College of Engineering & Research, Pune 411041, India
[c] Faculty of Periodontic, M. A. Rangoonwal College of Dental Science and Research Centre, Pune 411001, India
[d] International Clinical Dental Research Organization, Pune 411004, India

ARTICLE INFO

ABSTRACT

From the view of initial insertion of dental implant during implantation, the design of implants includes cylindrical, conical profile of implant body with number of cutting flutes at the tip of the implant. The current study aim was to investigate the effect of number of cutting flutes at the tip of the commercial dental implant system on stress distribution in cancellous bone. A three-dimensional CAD model is prepared and analyses using numerical simulation software. The significance of number of cutting flutes was studied under the applied load of 100 N axial (coronal-apical) direction, 40 N lateral (Bucco-lingual) direction and 100 N oblique at 45 degree to the longitudinal axis of the selected four types of implant system. A contact between implant and human jawbone is defined to model slide and stick conduct with coefficient of friction as 0.2 and the von Mises stress at the implant-bone interface in a cancellous bone is evaluated using ABAQUS numerical simulation code. The present study compared the effect of stress concentration at the location of implant cutting flutes and bone interface. The magnitude of von Mises stress (equivalent stress) for selected commercial dental implant system and the stress distribution pattern in a cancellous bone is analyzed. The implant system with number of cutting flutes is an acute parameter to effectively transfer the masticatory force and avoid the high stress concentration in cancellous bone at the interface.

© 2020 The Authors. Published by Elsevier Ltd.

1. Introduction

In the field of dentistry, the biocompatible pure titanium and titanium alloy dental implants are widely used in the human jaw mandible in place of missing tooth [1,2]. The primary stability is achieved by the percentage of bone and implants integrated with each other popularly known as osseointegration [3]. The biomechanical compatibility is one of the factors responsible for generating high stress at interface [4]. In literature primary stability of implantation depends on number of factors like quality and availability of human jawbone, design of implant geometry, clinical practices, and implantation postoperative treatments [5]. During

implantation easy insertion of implant and stable bone is more important. Implant geometry profile with number of cutting flutes is one of the crucial factors that affects the stress distribution along implant-bone interface [6–10].

Commercial dental implant manufacturer has a variety of implant design in size and shapes of implant profile with different shapes of cutting flutes [11]. Cutting flutes (CF) at the implant tip provides self-tapping ability during insertion [12]. Cutting flutes are necessary to reduce the heat during implantation and insertion torque [13]. It is important to know number of cutting flutes required along the interface for the rehabilitation success [14]. In order to understand the biomechanical significance of number of cutting flutes at the tip of the implant bonded with the surrounding bone, four implant system with a premolar region of mandibular jaw bone section were selected on the basis of literature review and questionnaire survey. A three-dimensional FE model is

* Corresponding author.
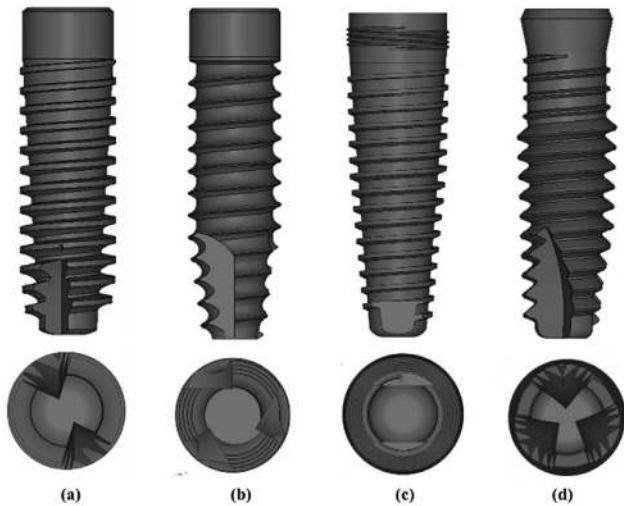 E-mail address: pankaj.dhatrak@mitwpu.edu.in (P. Dhatrak).

Fig. 1. Commercial Implant system front and bottom view showing the number of cutting flutes (a) IS-1with two cutting flutes (b) IS-2 with three cutting flutes (c) IS-3 with two cutting flutes and (d) IS-4 with three cutting flutes.

prepared using Hypermesh as a pre-processor and the ABAQUS code is used to evaluate the von-Mises stresses at the implant-bone interface [15].

2. Implant system

Four implant system (IS) with internal hex connection were selected viz. Ankylos (IS-1), Biohorizon (IS-2), Nobel (IS-3), and Xive (IS-4). The diameter and length of selected implant system (with various thread profile) were namely IS-1 (3.5 mm diameter, 14 mm length), IS-2 (3.4 mm diameter, 15 mm length), IS-3 (3.5 mm diameter, 14 mm length), and IS-4 (3.5 mm diameter, 15 mm length) [16].

3. Modeling and materials

3.1. CAD geometry modeling

The various profile dimensions like pitch, depth, height of thread, cutting flute profile of the selected dental implant were measured using Projector Profile measuring system [17] whereas the other major dimensions such as diameter, length, taper angle of implant is known from each implant system manufacturer. The implant, abutment, screw, and bone geometry are model using CreO CAD software. The implant system bone modeled as a cuboid shape of dimensions 25 mm height, 18 mm wide and 10 mm thick [6]. The cortical bone thickness is assumed to be 2 mm [18]. The detailed CAD model with cutting flutes of each implant system is shown in the Fig. 1.

3.2. Finite element modeling (FE Modeling)

3.2.1. FE mesh modeling

To perform the numerical simulation, a quadratic 3D tetrahedral element is used to model the implant, abutment, screw and bone with average element size of 0.1 mm whereas the premolar dental crown has been modeled with linear quadrilateral element with average size of 0.2 mm. Mesh convergence is mainly depends on the number of element and the mesh structure [19,20]. The cut-section of implant prosthetic mesh refinement at different contact zone (Fig. 2(b)) were used to control numerical simulation time [21,22]. The cortical and cancellous bone near the implant surface is modelled with fine mesh to accurately capture the stresses whereas the bone area away from the interface is modelled with coarse mesh as shown in Fig. 2(c). The total number of elements and nodes in selected implant system is approximately 671000-847000 and 144000-177000 respectively shown in Table 1.

3.2.2. Implant-bone zone

Implant stability is achieved by means of implant thread profile surface bonded with surrounding bone tissues along the implant-bone interface [23]. A friction contact is defined to simulate the implant-bone interface condition [24,25]. In the current study, the implant-cancellous bone and the implant-cortical bone inter-

Table 1
FE entities in the implant system.

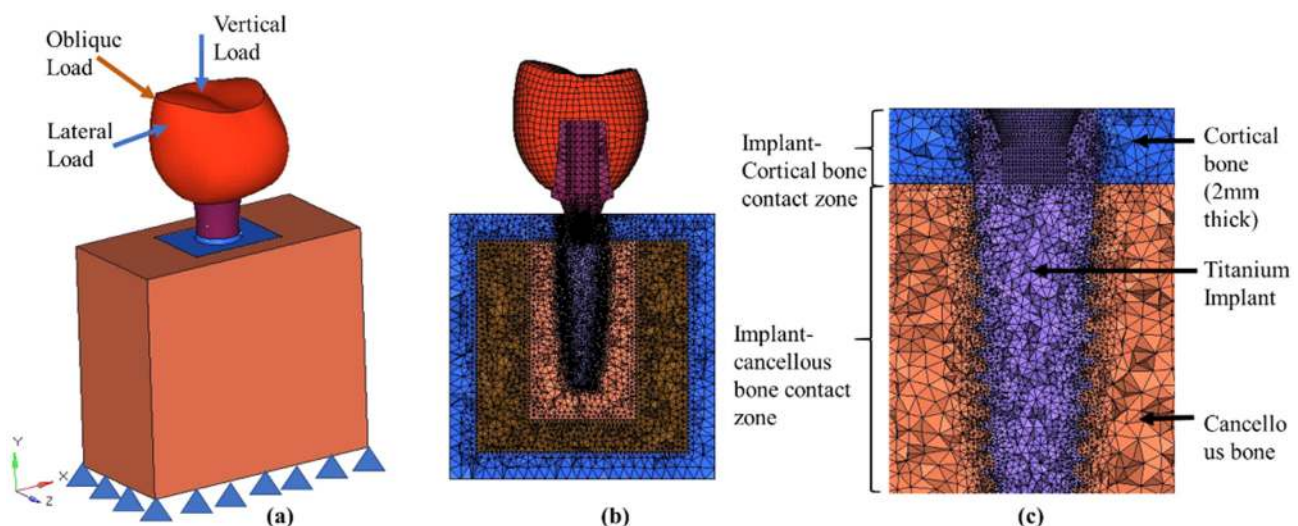| Implant system	Number of elements	Number of nodes
IS-1	671,000	144,000
IS-2	783,000	158,000
IS-3	837,000	167,000
IS-4	847,000	177,000

Fig. 2. FE model of implant system (a) loads and boundary condition applied on implant system (b) Cut section of mesh model of implant with bone (c) Mesh enhancement at the interface.

Table 2
Mechanical Properties of Implant System.

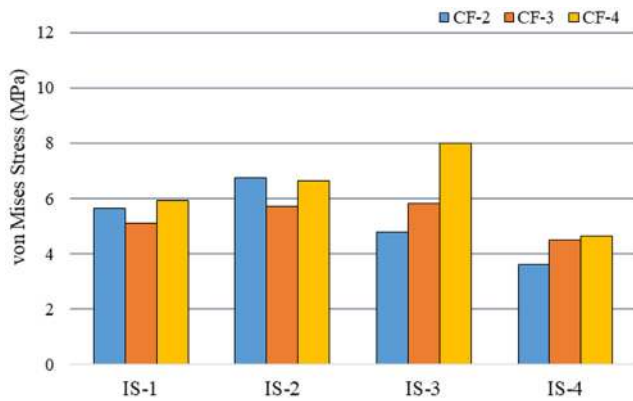| Implant system components	Materials	E (MPa)	μ	References
Implant, Abutment and Screw	Titanium alloy	110,000	0.33	[9,21,27]
Hard jawbone	Cortical bone	13,700	0.26	[2,14,27]
Soft jawbone	Cancellous bone	1370	0.31	[14,21]
Crown	Porcelain	70,000	0.19	[9]

Fig. 3. von Mises stress results comparison between numbers of cutting flutes under 100 N vertical load.

Fig. 5. von Mises stress results comparison between numbers of cutting flutes under 100 N oblique 45° load.
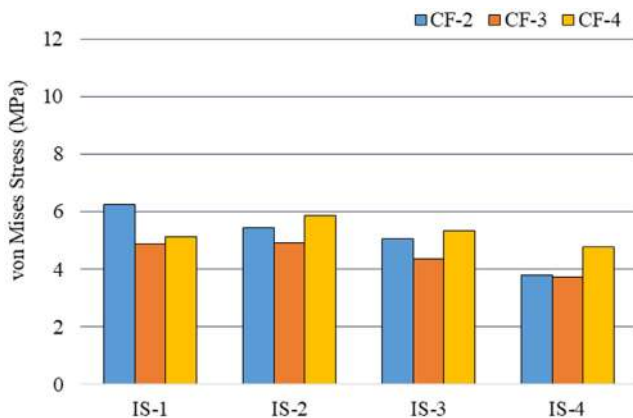

Fig. 4. von Mises stress results comparison between numbers of cutting flutes under 40 N Lateral load.

face is modeled as nonlinear contact zone with coefficient of friction is consider as 0.2 in a numerical simulation [18] whereas the implant-abutment, abutment-screw, screw-implant, abutment-crown interface is considered to be a rigid [26].

3.2.3. Mechanical properties

Titanium alloy (Grade IV – Ti-6Al-4V) widely utilized as biocompatible material in the field of implant dentistry. The mechanical properties such as Young's Modulus (E), Poisson Ratio (μ) of implant system components are shown in Table 2.

3.2.4. Load and boundary conditions

Vertical and lateral forces mainly induce due to mastication and horizontal motion of the mandible. Based on previous literature three loading conditions were simulated in FE simulation [22,28–30]. Masticatory forces induced compressive force whereas transverse forces were induced due to position of tooth cups and horizontal movement of the mandible [31]. An occlusal tooth in
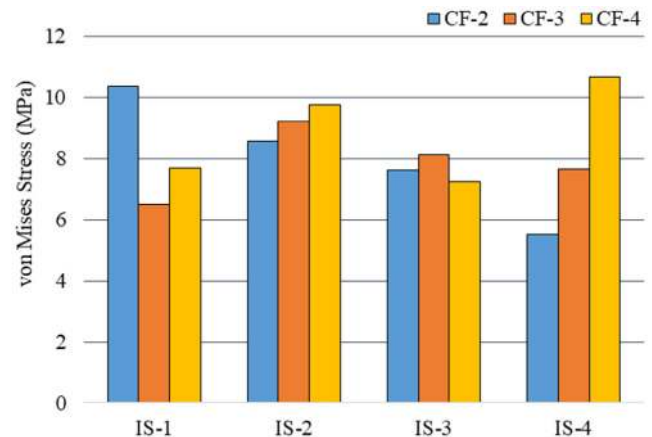
contact normally results in 3-directional forces defined in the present study. A vertical compressive load (mastication force) of 100 N [32,33] along the axis of implant, lateral load (lateral movement of mandible during mastication) of 40 N [34] in Bucco-lingual direction (cheek-tongue direction) and an oblique load (100 N) at 45° inclination to longitudinal axis of implant (due to motion of mandible & inclination of tooth cusps) [35–37] were applied to occlusal plane of the crown to analyze the stress distribution in the cancellous bone in the vicinity of implant-bone interface. The oblique load is applied as a vertical and horizontal component of force on the crown surface. The bottom and lateral side bone nodes of FE model were constraints in 3 directions with degree of freedom zero. A contact stress analysis was performed using Abaqus software [38,39] with loads and constraints shown in Fig. 2(a).

4. Result and discussion

Self-tapping capability of implant tip is improved using cutting flutes [13]. In the present study the commercial model IS-1 and IS-3 has two cutting flutes (CF-2) and model IS-2 and IS-4 has three cutting flutes (CF-3). Implant flute design consists of some variables, which includes shape of flutes, length, depth, and number of flutes. All design iteration with change in number of cutting flutes were compared with the original cutting flutes provided at the tip of implant. Comparison between the selected dental implant system for von Mises stress results under applied vertical load, lateral load and oblique load are presented in Figs. 3–5, respectively.

In Model IS-1 (CF-2) the von Mises stress in the cancellous bone near the flutes and bone interface under 100 N vertical, 40 N lateral and 100 N oblique were 5.64, 6.25 and 10.38 MPa respectively (Fig. 6). These stresses were 10.8–59.9% larger than CF-3 models while 22–35.15% larger than CF-4 models, except vertical loading conditions. In Model IS-2 (CF-3) the von Mises stress in the cancellous bone near the flutes and bone interface under 100 N vertical, 40 N lateral and 100 N oblique were 5.72, 4.91 and 9.22 MPa
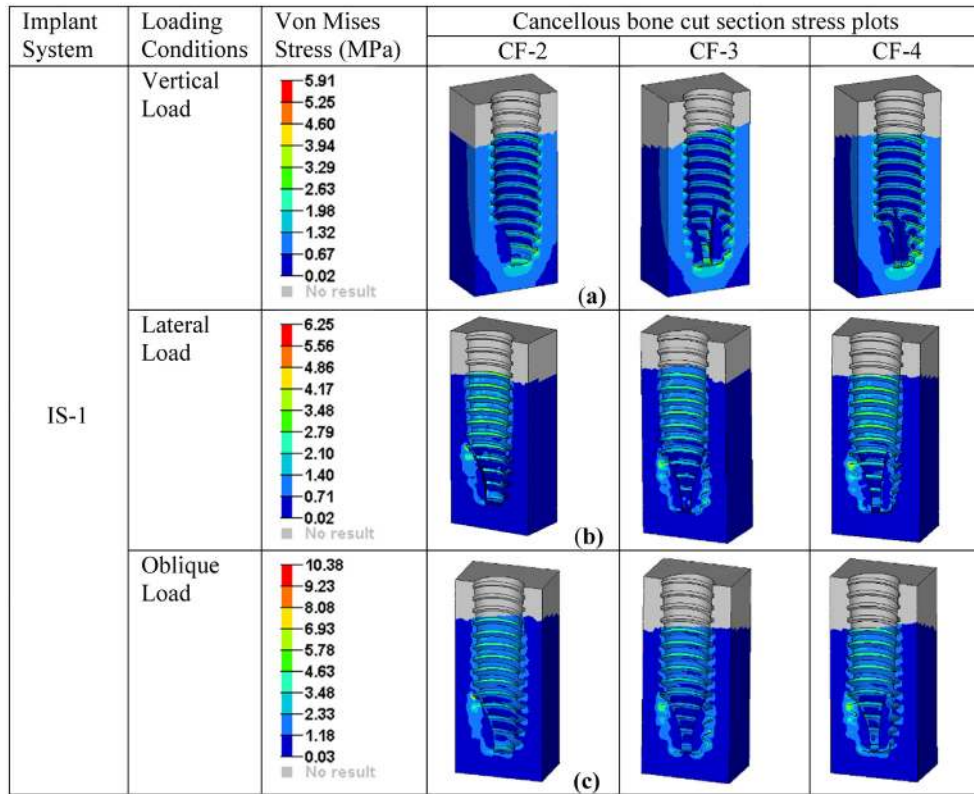
Implant System	Loading Conditions	Von Mises Stress (MPa)	Cancellous bone cut section stress plots		
			CF-2	CF-3	CF-4
IS-1	Vertical Load	5.91 / 5.25 / 4.60 / 3.94 / 3.29 / 2.63 / 1.98 / 1.32 / 0.67 / 0.02 / No result			(a)
	Lateral Load	6.25 / 5.56 / 4.86 / 4.17 / 3.48 / 2.79 / 2.10 / 1.40 / 0.71 / 0.02 / No result			(b)
	Oblique Load	10.38 / 9.23 / 8.08 / 6.93 / 5.78 / 4.63 / 3.48 / 2.33 / 1.18 / 0.03 / No result			(c)

Fig. 6. Cancellous bone (cut-section view) showing von Mises stress distribution near cutting flutes implant-bone interface of original Implant system (IS-1) under vertical (a), lateral (b) and oblique load (c).

Implant System	Loading Conditions	Von Mises Stress (MPa)	Cancellous bone cut section stress plots		
			CF-2	CF-3	CF-4
IS-2	Vertical Load	6.76 / 6.01 / 5.26 / 4.51 / 3.75 / 3.00 / 2.25 / 1.50 / 0.75 / 0.00 / No result			(a)
	Lateral Load	5.86 / 5.21 / 4.56 / 3.91 / 3.26 / 2.61 / 1.96 / 1.31 / 0.66 / 0.01 / No result			(b)
	Oblique Load	9.77 / 8.69 / 7.61 / 6.53 / 5.45 / 4.36 / 3.28 / 2.20 / 1.12 / 0.04 / No result			(c)

Fig. 7. Cancellous bone (cut-section view) showing von Mises stress distribution near cutting flutes implant-bone interface of original Implant system (IS-2) under vertical (a), lateral (b) and oblique load (c).
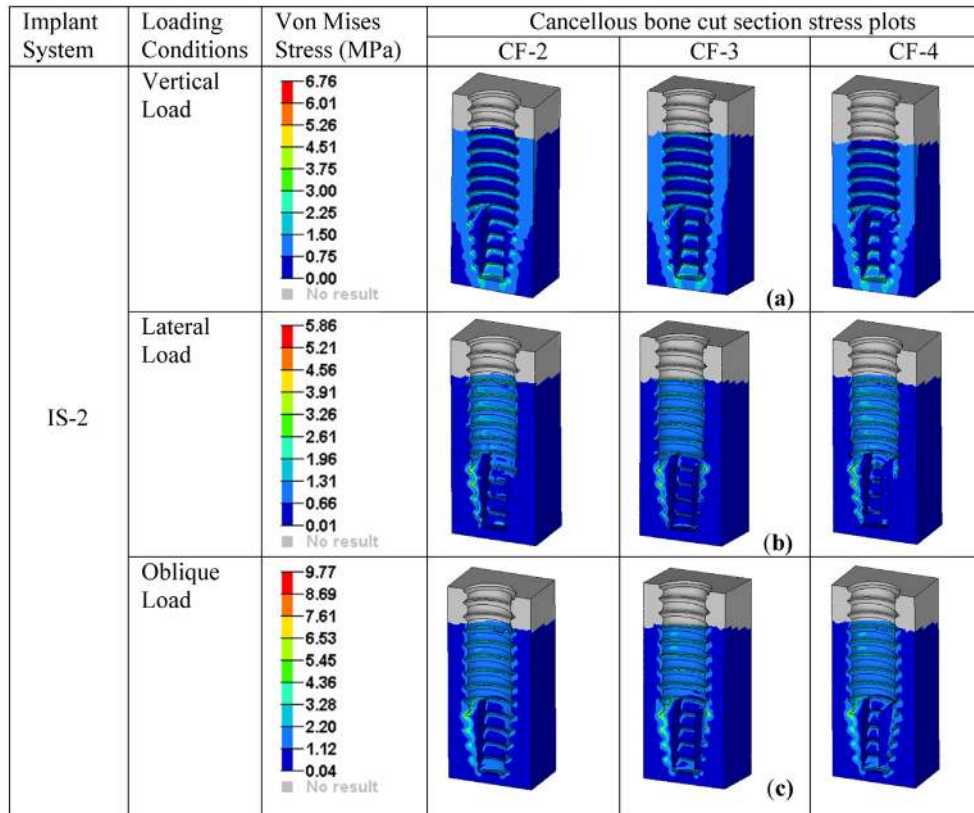
Fig. 8. Cancellous bone (cut-section view) showing von Mises stress distribution near cutting flutes implant-bone interface of original Implant system (IS-3) under vertical (a), lateral (b) and oblique load (c).
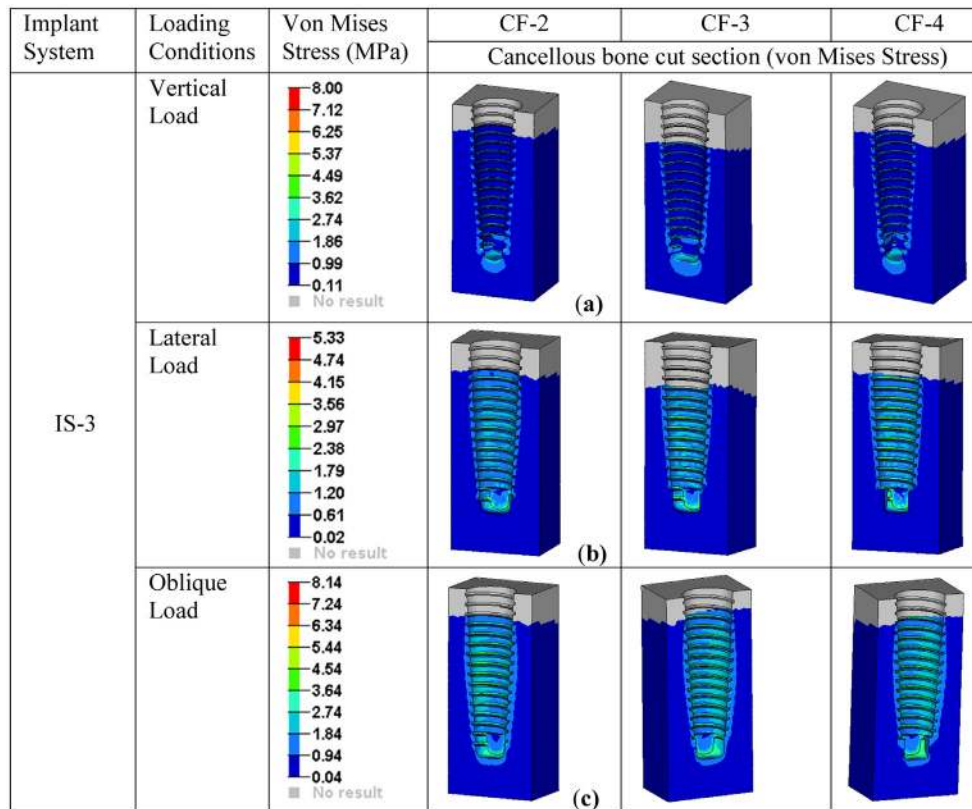
respectively (Fig. 7). Shu-Wei Wu et al. [12] study shows that insertion torque value of the nonfluted implant is considerably higher than that of the fluted implant which ultimately increase the stress at bone level. The von Mises stress in the cancellous bone near the flutes and bone interface under 100 N vertical and 40 N lateral is increased by 18.1 and 15.9% in comparison with model CF-2 and CF-4 respectively while 100 N oblique it will decrease by 6.94% in model CF-2 and increased by 5.9% in model CF-4.

In Model IS-3 (CF-2) the von Mises stress in the cancellous bone near the flutes and bone interface under 100 N vertical, 40 N lateral and 100 N oblique were 4.77, 5.04 and 7.61 MPa respectively (Fig. 8). The von Mises stress in the cancellous bone near the flutes and bone interface under 100 N oblique load (Fig. 5) is decreased by 6.5% with model CF-3 but its eventually reduce the primary stability [23] and increased by 5.1% with model CF-4 whereas under lateral load (Fig. 4) it is increased by 16.1% in model CF-3 and decreased by 5.4% with model CF-4. Under vertical load (Fig. 7) the von Mises stress value is decreased by 18.1 and 40.3% with model CF-3 and CF-4 respectively. In Model IS-4 (CF-3) the von Mises stress in the cancellous bone near the flutes and bone interface under 100 N vertical, 40 N lateral and 100 N oblique were 4.51, 3.74 and 7.65 MPa respectively (Fig. 9). The von Mises stress in the cancellous bone near the flutes and bone interface under 100 N vertical (Fig. 3) and 100 N oblique (Fig. 5) were larger than 38.5 and 24.9% than model CF-2. Similarly, the stress values were smaller than 3.0 and 28.3% with model CF-4.

In one of the comparative study by Jimbo R. et al. [40] shows that, the implant with a modified cutting flute design significantly reduced the insertion torque compared to implants with a traditional cutting flutes thread, and resulted in a different healing pattern that may be beneficial to improve stability. Compared with all three cutting flutes model in the present study, IS-2 and IS-3 shows minimum stress difference at the interface under oblique and lateral loading. Similarly, model IS-1, IS-2 and IS-4 shows minimum stress variation at the interface under vertical loading. The model IS-1 and IS-4 under oblique loads and model IS-3 under vertical load shows large variation in the stress near the cutting flutes implant-bone interface.

5. Conclusions

Present study compared the von Mises stress results obtained from original cutting flutes models with those simulated for the range of number of cutting flutes from numerical analysis. The maximum von Mises stress is concentrated near the cutting flutes zone during the masticatory force. The influence of number of cutting flutes of all selected implant system on stress distribution pattern at implant-bone interface was evaluated. Stress distribution in all models of implant system at the interface near the cutting flutes appeared to be symmetrical under all loading conditions. Stress in the model IS-3 (CF-2) is much smaller than the model CF-4 under applied vertical load. IS-4 (CF-3) system shows minimum stress with the model CF-2. Similarly, IS-2 (CF-3) system shows minimum stress under oblique loading condition. Implant system with CF-4 is not recommended as it gives higher stress concentration at the bone-implant interface near the cutting flutes. From the present study though the cutting flutes helps in implantation, still implant system with two cutting flutes (CF-2) is recommended as it will produce less stress concentration at the interface near the cutting flutes edges. The implant system with number of cutting flutes is an acute parameter to effectively transfer the masticatory force and avoid the high stress concentration region into cancellous bone.
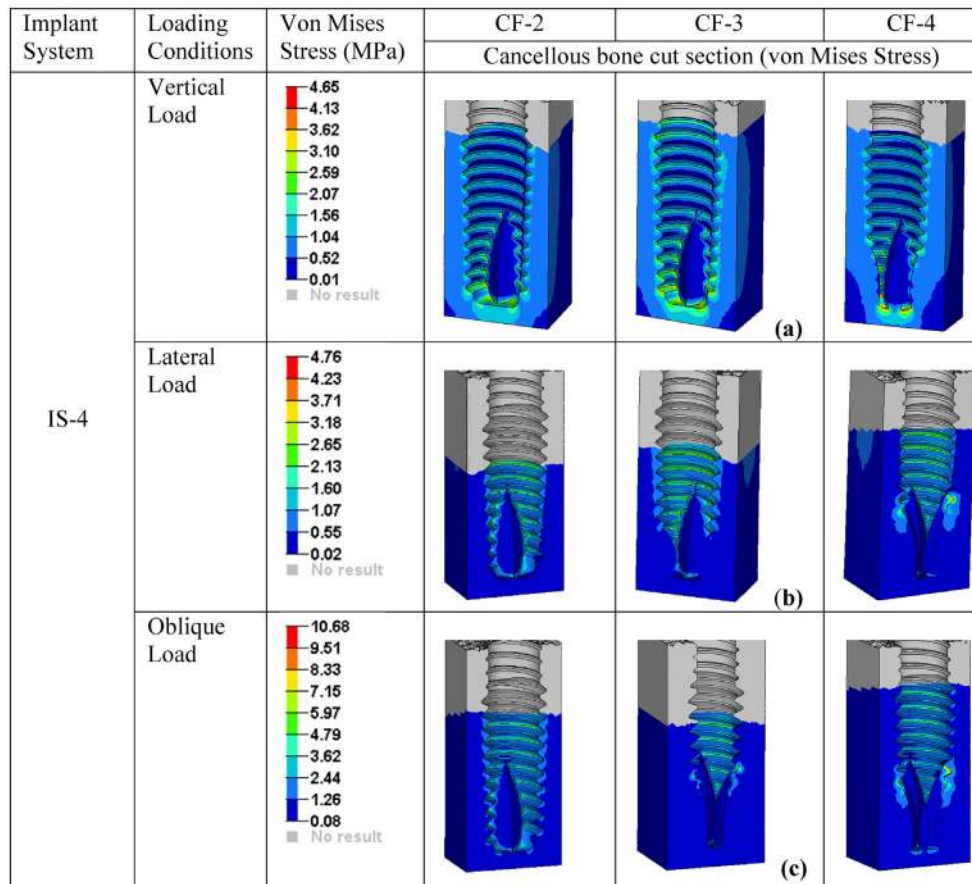
P. Dhatrak et al.

Fig. 9. Cancellous bone (cut-section view) showing von Mises stress distribution near cutting flutes implant-bone interface of original Implant system (IS-4) under vertical (a), lateral (b) and oblique load (c).

CRediT authorship contribution statement

Pankaj Dhatrak: Conceptualization, Data curation, Formal analysis, Investigation, Methodology, Resources, Software, Validation, Writing - original draft. **Uddhav Shirsat:** Investigation, Project administration, Supervision, Visualization, Writing - review & editing. **S. Sumanth:** Data curation, Methodology, Visualization. **Vijay Deshmukh:** Methodology, Writing - review & editing.

Declaration of Competing Interest

The authors declare that they have no known competing financial interests or personal relationships that could have appeared to influence the work reported in this paper.

Acknowledgement

References

[1] S. Faegh, S. Muftu, Load transfer along the bone–dental implant interface, J. Biomech. 43 (2010) 1761–1770.

[2] R. Vayron, V.-H. Nguyen, R. Bosc, S. Naili, G. Haiat, Finite element simulation of ultrasonic wave propagation in a dental implant for biomechanical stability assessment, Biomech. Model. Mechanobiol. (2015), doi: 10.100/s 10237-015-0651-7.

[3] S.-K. Chien, S.-S. Hsue, C.-S. Lin, T.-F. Kuo, D.-J. Wang, Jen-Chang Yang, Sheng-Yang Lee, Influence of threaded design on dental implant osseointegration assayed using the lan-yu mini-pig model, J. Med. Biol. Eng. (2017), https://doi.org/10.1007/s40846-017-0240-6.

[4] M. Shi, H. Li, X. Liu, Multidisciplinary design optimization of dental implant based on finite element method and surrogate models, J. Mech. Sci. Technol. 31 (10) (2017) 5067–5073.

[5] Pankaj Dhatrak, Uddhav Shirsat, Vijay Deshmukh, Sumanth S., 2018, Fatigue Life Prediction of commercial dental implant using analytical approach and verification by FEA, Proceedings of Fatigue, Durability and Fracture Mechanics, Lecture Notes in Mechanical Engineering 203-212, https://doi.org/10.1007/978-981-10-6002-1_16. (2018).

[6] S. Kamal Jalali, R. Yarmohammadi, F. Maghsoudi, Finite element stress analysis of functionally graded dental implant of a premolar tooth, J. Mech. Sci. Technol. 30 (11) (2016) 4919–4923, https://doi.org/10.1007/s12206-016-1011-y.

[7] M. Ghadiri, N. Shafiei, Sadegh Hemmati Salekdeh, Parya Mottaghi, Tahereh Mirzaie, Investigation of the dental implant geometry effect on stress distribution at dental implant-bone interface, J. Braz. Soc. Mech. Sci. Eng. (2016), https://doi.org/10.1007/s40430-015-0472-8.

[8] P. Ausiello, P. Franciosa, M. Martorelli, D.C. Watts, Effects of thread features in osseo-integrated titanium implants using a statistics-based finite element method, Dent. Mater. 28 (2012) 919–927.

[9] J. Chen, Z. Zhang, X. Chen, C. Zhang, G. Zhang, X.u. Zhewu, Design and manufacture of customized dental implants by using reverse engineering and selective laser melting technology, J. Prosth. Dentis. 112 (5) (2014) 1088–1095.

[10] T. Li, K. Hub, L. Cheng, Y. Ding, Y. Ding, J. Shao, L. Kong, Optimum selection of the dental implant diameter and length in the posterior mandible with poor bone quality – A 3D finite element analysis, Appl. Math. Model. 35 (2011) 446–456.

[11] H. Abuhussein, G. Pagni, A. Rebaudi, H.L. Wang, The effect of thread pattern upon implant osseointegration, Clin. Oral Implant Res. 21 (2010) 129–136, https://doi.org/10.1111/j.1600-0501.2009.01800.x.

[12] W.u. Shu-Wei, C.C. Lee, F.u. Ping-Yuen, S.C. Lin, The effects of flute shape and thread profile on the insertion torque and primary stability of dental implants, J. Med. Eng. Phys. 34 (2012) 797–805.

[13] M.B. Bickley, D.P. Hanel, Self-tapping versus standard tapped titanium screw fixation in the upper extremity, J. Hand Surg. 23 (2) (1998) 308–311.

[14] Marcelo Bighetti Toniollo, Ana A three-dimensional finite element analysis of the stress distribution on morse taper implants surface, J. Prosthodon. Res. 57 (3) (2013) 206–212.

P. Dhatrak et al.

[15] ABAQUS, Version 6.7 Documentation, ABAQUS Analysis Manual, Simulia, Dassault Systems, RI, USA 2007.
[16] P. Dhatrak, U. Shirsat, S. Sumanth, V. Deshmukh, Finite element analysis and experimental investigations on stress distribution of dental implants around implant-bone interface, Mater. Today. Proc. 5 (2018) 5641–5648.
[17] Pankaj Dhatrak, Uddhav Shirsat, Vijay Deshmukh, Sumanth S., (2018), Fatigue Life Prediction of commercial dental implant using analytical approach and verification by FEA, Proceedings of Fatigue, Durability and Fracture Mechanics, Lecture Notes in Mechanical Engineering 203-212.
[18] H.C. Chang, H.Y. Li, Y.N. Chen, C.H. Chang, C.H. Wang, Mechanical analysis of a dental implant system under 3 contact conditions and with 2 mechanical factors, J. Prosthet. Dent. 122 (4) (2019) 376–382.
[19] L. Kong, Y. Sun, H.u. Kaijin, Y. Liu, D. Li, Z. Qiu, B. Liu, Selections of the cylinder implant neck taper and implant end fillet for optimal biomechanical properties: a three-dimensional finite element analysis, J. Biomech. 41 (2008) 1124–1130.
[20] A. Jarrahi, H. Asgharzadeh Shirazi, A. Asnafi, M.R. Ayatollahi, J. Braz. Soc. Mech. Sci. Eng. 40 (249) (2018), https://doi.org/10.1007/s40430-018-1166-9.
[21] B. Piotrowski, A.A. Baptista, E. Patoor, P. Bravetti, A. Eberhardt, P. Laheurte, Interaction of bone-dental implant with new ultra-low modulus alloy using a numerical approach, Mater. Sci. Eng. C 38 (2014) 151–160.
[22] L.u. Songhe, T. Li, Y. Zhang, L.u. Chunlei, Y. Sun, Biomechanical optimization of the diameter of distraction screw in distraction implant by three-dimensional finite element analysis, Comput. Biol. Med. 43 (2013) 1949–1954.
[23] V. Mathieu, R. Vayron, G. Richard, G. Lambert, S. Naili, J.-P. Meningaud, G. Haiat, Biomechanical determinants of the stability of dental implants: Influence of the bone-implant interface properties, J. Biomech. 47 (2014) 3–13.
[24] S.H. Chang, C.L. Lin, S.S. Hsue, Y.S. Lin, S.R. Huang, Biomechanical analysis of the effects of implant diameter and bone quality in short implants placed in the atrophic posterior maxilla, Med. Eng. Phys. 34 (2012) 153–160.
[25] J. Wolff, N. Narra, A.-K. Antalainen, J. Valasek, J. Kaiser, G.K. Sandor, P. Marcian, Finite element analysis of bone loss around failing implants, Mater. Des. 61 (2014) 177–184.
[26] Aaron Yu-Jen Wu, Jui-Ting Hsu, Winston Chee, Yun-Te Lin, Lih-Jyh Fuh, Heng-Li Huang, Biomechanical evaluation of one-piece and two piece small-diameter dental implants: In-vitro experimental and three-dimensional finite element analyses, J. Formos. Med. Assoc. 115 (2016) 794–800.
[27] Heng-Li Huang, Ming-Tzu Tsai, Jui-Ting Hsu, Lih-Jyh Fuh, Ming-Gene Tu and Aaron Yu-Jen Wu, Do Threaded Size and Surface Roughness Affect the Bone Stress and Bone-Implant Interfacial Sliding of Titanium Dental Implant?, Proceedings of the World Congress on Engineering 2011 Vol III WCE 2011, July 6-8, 2011, London, U.K.
[28] I. Hasan, B. Roger, F. Heinemann, L. Keilig, C. Bourauel, Influence of abutment design on the success of immediately loaded dental implants: experimental and numerical studies, Med. Eng. Phys. 34 (2012) 817–825.
[29] Eduardo Piza Pellizzer, Caroline Cantieri de Mello, Joel Ferreira Santiago Junior, Victor Eduardo de Souza Batista, Daniel Augusto de Faria Almeida, Fellippo Ramos Verri, Analysis of the biomechanical behavior of short implants: The photo-elasticity method, Materials Science and Engineering C 55 (2015) 187–192.
[30] F. Lofaj, J. Kucera, D. Nemeth, L. Kvetkova, Finite element analysis of stress distributions in mono- and bi-cortical dental implants, Mater. Sci. Eng., C 50 (2015) 85–96.
[31] Misch C. Contemporary Implant dentistry. 3rd Editio. St. Louis, Mosby Inc.; 2007.
[32] M.J. Hisam, I. Zaman, S. Sharif, D. Kurniawan, F.M. Nor, Finite element analysis of mini implant biomechanics on peri-implant bone, Procedia Manuf. 30 (2019) 308–314, https://doi.org/10.1016/j.promfg.2019.02.044.
[33] M. M. A. Peyroteo, H. I. G. Gomes, J. Belinha, and R. M. N. Jorge, Biomechanical analysis of bone tissue after insertion of dental implants using meshless methods: Stress analysis and osseointegration. Elsevier Inc., (2019).
[34] M. Shash, H. Nazha, W. Abbas, Influence of different abutment designs on the biomechanical behavior of one-piece zirconia dental implants and their surrounding bone: a 3D-FEA, Irbm 40 (6) (2019) 313–319, https://doi.org/10.1016/j.irbm.2019.07.001.
[35] M.R. Niroomand, M. Arabbeiki, Implant stability in different implantation stages: analysis of various interface conditions, Inform. Med. Unlocked 19 (2020), https://doi.org/10.1016/j.imu.2020.100317 100317.
[36] A. Brune, M. Stiesch, M. Eisenburger, A. Greuling, The effect of different occlusal contact situations on peri-implant bone stress – A contact finite element analysis of indirect axial loading, Mater. Sci. Eng C 99 (2019) 367–373, https://doi.org/10.1016/j.msec.2019.01.104.
[37] A. M. O. Dal Piva et al., "Short communication: Influence of retainer configuration and loading direction on the stress distribution of lithium disilicate resin-bonded fixed dental prostheses: 3D finite element analysis," J. Mech. Behav. Biomed. Mater., vol. 100, no. May, (2019), doi: 10.1016/j.jmbbm.2019.103389.
[38] H. Lee, S. Park, G. Noh, Biomechanical analysis of 4 types of short dental implants in a resorbed mandible, J. Prosthet. Dent. 121 (4) (2019) 659–670, https://doi.org/10.1016/j.prosdent.2018.07.013.
[39] M. Pirmoradian, H.A. Naeeni, M. Firouzbakht, D. Toghraie, M., K., khabaz,, and, R., Darabi,, Finite element analysis and experimental evaluation on stress distribution and sensitivity of dental implants to assess optimum length and thread pitch, Comput. Methods Programs Biomed. 187 (2020), https://doi.org/10.1016/j.cmpb.2019.105258 105258.
[40] R. Jimbo et al., The impact of a modified cutting flute implant design on osseointegration, Int. J. Oral Maxillofac. Surg. 43 (7) (2014) 883–888, https://doi.org/10.1016/j.ijom.2014.01.016.